

Pretargeted Radioimmunotherapy of Human Colorectal Xenografts with Bispecific Antibody and ^{131}I -Labeled Bivalent Hapten

Emmanuel Gautherot, Eric Rouvier, Laurent Daniel, Eric Loucif, Jamila Bouhou, Corine Manetti, Marie Martin, Jean-Marc Le Doussal, and Jacques Barbet

Immunotech SA, Marseille; Laboratoire de Biopathologie Nerveuse et Musculaire, Université de Provence, Faculté de Médecine, Marseille; and Laboratoire d'Immunologie Cellulaire, Hôpital Pitié-Salpêtrière, Paris, France

We have developed a pretargeting strategy, called the affinity enhancement system (AES), which uses bispecific antibodies to target radiolabeled bivalent haptens to tumor cells. The aim of this study was to evaluate the potential of the AES for the radioimmunotherapy (RIT) of LS174T colorectal xenografts in comparison with RIT with directly labeled $\text{F}(\text{ab}')_2$ fragment. **Methods:** A total of 6 groups of tumor-bearing mice were treated using anticarcinoembryonic antigen (CEA) \times anti-diethylenetriamine pentaacetic acid (DTPA)-In bispecific antibody ($\text{BsF}(\text{ab}')_2$) and ^{131}I -labeled di-DTPA-In bivalent hapten. Three groups of mice were injected with various activities of ^{131}I -labeled bivalent hapten (75, 96, and 112 MBq) 20 h after administration of $\text{BsF}(\text{ab}')_2$. Three other groups were injected with an almost constant activity of labeled hapten (102 MBq) at 3 time periods (15, 30, and 48 h) after $\text{BsF}(\text{ab}')_2$ administration. For conventional RIT, mice were treated with 96 MBq ^{131}I -labeled anti-CEA $\text{F}(\text{ab}')_2$. Control groups were left untreated. Toxicity and tumor growth were monitored at weekly intervals. **Results:** Doses used for conventional RIT induced severe toxicity and resulted in death of several treated animals. Nevertheless, all surviving animals treated with ^{131}I -labeled anti-CEA $\text{F}(\text{ab}')_2$ relapsed shortly after treatment (tumor growth delay = 48 ± 13 d). For animals treated with the AES reagents, toxicity varied with the pretargeting time interval and the administered activity. For 20-h pretargeting time, the maximum tolerated dose was 96 MBq. For all AES RIT except 1 (with 48-h pretargeting time interval and growth delay of 82 ± 26 d), no tumor growth was observed over a period of 8 mo. Furthermore, based on clinical and histologic criteria, 33% of the treated mice were considered cured. **Conclusion:** High cure rates of LS174T colon carcinoma were achieved with the AES, and the flexibility of the pretargeting approach allowed the control of hematologic toxicity, which is the main limitation to dose escalation with conventional RIT.

Key Words: radioimmunotherapy; pretargeting; colorectal carcinoma; bispecific antibody; ^{131}I

J Nucl Med 2000; 41:480–487

Radioimmunotherapy (RIT) with ^{131}I -labeled monoclonal antibodies has given contrasting clinical results. In the

treatment of refractory B-cell lymphomas, complete cures have been achieved (1,2). In solid tumors, because of poor accessibility and lower radiosensitivity, only partial responses have been reported (3–6). A major limitation of RIT in solid tumors is secondary toxicity, especially to the hematopoietic system. Several approaches to improving tumor-to-normal organ ratios, based on the pretargeting concept, are under investigation (7,8).

We have developed a pretargeting strategy, the affinity enhancement system (AES), which uses bispecific antibodies to target radiolabeled bivalent haptens to antigens at the surface of tumor cells. The bivalent hapten is injected after a delay, which allows excess bispecific antibody to clear from circulation. In addition, the bivalence of the hapten explains its higher avidity for cell-bound than for free-circulating bispecific antibody ($\text{BsF}(\text{ab}')_2$) through cooperative binding at the cell surface (9). In experimental tumors in mice, the AES achieved fast and high activity uptake in the tumor, long tumor residence time, and contrast ratios to most normal organs 2–3 times greater than those obtained with directly labeled antibodies or fragments (9–12). These features have been confirmed in clinical trials with immunoscintigraphy of carcinoembryonic antigen (CEA)-expressing tumors (13–15). Furthermore, a preliminary clinical dosimetry study has shown that ^{131}I -labeled AES reagents could deliver radiation doses to tumors in the range of those obtained using direct targeting, but with reduced exposure of normal organs (16).

The aim of this study was to evaluate the application of the AES to RIT of a CEA-expressing solid tumor in an animal model. Therefore, ^{131}I -labeled bivalent diethylenetriamine pentaacetic acid (DTPA) hapten targeted by anti-CEA \times anti-DTPA-In $\text{BsF}(\text{ab}')_2$ was compared with ^{131}I -labeled anti-CEA $\text{F}(\text{ab}')_2$ for the treatment of nude mice grafted with LS174T human colorectal carcinoma. The results are discussed with respect to therapeutic efficiency and treatment toxicity.

MATERIALS AND METHODS

Tumor Model

Female NMRI nu/nu mice, 10–12 wk old, were obtained from CERJ (Laval, France). The human colon carcinoma LS174T cell

Received Jan. 25, 1999; revision accepted Jun. 21, 1999.
For correspondence or reprints contact: Emmanuel Gautherot, PhD, Antibody Department, Immunotech SA, 130 Avenue De Lattre de Tassigny, BP 177 13276, Marseille Cedex 9, France.

line (ATCC, Rockville, MD) was grown as reported (12). Tumor cells (2.5×10^6) were grafted in nude mice by subcutaneous injection in the flank. Ten days later, mice were selected for experiments.

Monoclonal Antibodies and Preparation of Bispecific Antibodies

Anti-CEA clone F6 (Immunotech, Marseille, France), anti-DTPA-In clone 734 (9) (Immunotech), anti-high-molecular-weight melanoma-associated antigen (HMW-MAA) clone G7A5 (obtained from Dr. J.F. Doré, INSERM, Lyon, France), antihistamine clone 679.1MC7 (17) (Immunotech), and anti-F6 idiotype clone 44.12.13 (Immunotech) are mouse IgG1s. All antibodies were purified from ascites fluid by affinity chromatography on protein A-Sepharose (Pharmacia, Uppsala, Sweden). F(ab')₂ fragments were prepared by digestion with pepsin (Sigma Chemical Co., St. Louis, MO). The bispecific antibodies were prepared by coupling reduced F(ab')₂ with *o*-phenylenedimaleimide (Sigma) as reported (18). The 100-kDa fraction corresponding to the bispecific antibody (BsF(ab')₂) was purified by gel filtration on a Superdex 200 column (Pharmacia).

Bivalent Hapten

N α -DTPA-tyrosyl-N ϵ -DTPA-lysine was synthesized as described (9).

Labeling

Anti-CEA F6 F(ab')₂ was labeled using Iodo-Gen (Pierce, Rockford, IL) with 370 MBq Na¹³¹I (180–220 MBq/ μ g; CIS Bio International, Saclay, France) for 6 nmol protein.

The bivalent hapten was labeled with iodine using chloramine-T as follows: 15 nmol of indium chloride-saturated hapten were iodinated with 1.5 GBq Na¹³¹I and 50 μ g chloramine-T. The reaction was stopped after 2 min at room temperature by adding 100 μ g sodium disulfide and incubated for 5 min at room temperature. The labeled hapten was then purified on a SepPak C₁₈ cartridge (Millipore, Milford, MA) equilibrated in 1 mol/L N-[2-hydroxyethyl]piperazine-N'-[2-ethanesulfonic acid], pH 8.0, and eluted in 100% methanol. The methanol was evaporated in a rotary evaporator at 65°C for 30–45 min. The final solution of labeled hapten was then adjusted to 8 mmol/L cysteamine to avoid radiolysis.

RIT Experiments

The average tumor volume selected for experiments was 129 ± 103 mm³ (32–470 mm³). Each group of treated mice had its own untreated control group. A total of 6 groups of 10–12 mice were treated using anti-CEA \times anti-DTPA-In F6–734 BsF(ab')₂ and ¹³¹I-labeled di-DTPA-In bivalent hapten. Two sets of experiments were performed. In the first, the pretargeting time was kept constant (at 20 h), whereas the injected activity of labeled bivalent hapten was set at 2.9 ± 0.2 , 3.4 ± 0.4 , and 3.8 ± 0.3 MBq/g, resulting in respective total activities of 75.5 ± 3.0 , 96.2 ± 8.1 , and 112.5 ± 1.8 MBq. These groups are referred to as AES 20/2.9, AES 20/3.4, and AES 20/3.8. In the second set of experiments, an almost constant activity of labeled hapten (3.8 ± 0.4 , 3.9 ± 0.3 , and 3.7 ± 0.5 MBq/g; total activities of 97.9 ± 2.4 , 111.2 ± 1.6 , and 96.3 ± 0.5 MBq) was injected after various pretargeting delays (15, 30, and 48 h, respectively) after administration of the BsF(ab')₂. These groups are referred to as AES 15/3.8, AES 30/3.9, and AES 48/3.7, respectively. The protein dose of BsF(ab')₂ ranged from 2.4 to 3 nmol, and the bivalent hapten-to-BsF(ab')₂ molar ratio was set to

0.5. As a control for the effect of nonspecific hapten targeting, a group of mice (AES controls) was injected with the same number of anti-CEA and anti-DTPA-In binding sites but carried by 2 distinct BsF(ab')₂ (6 nmol equimolar mixture of anti-CEA \times antihistamine (F6–679) and anti-HMW-MAA \times anti-DTPA-In (G7A5–734) BsF(ab')₂) and 15 h later with 3.6 ± 0.3 MBq/g (89.2 ± 1.2 MBq) ¹³¹I-labeled di-DTPA-In. In a final experiment, 8 nude mice without tumors were injected with 3.5 ± 0.3 MBq/g (74.9 ± 3.7 MBq) bivalent hapten. For conventional RIT, 10 mice were injected with 3.7 ± 0.4 MBq/g (96.1 ± 5.0 MBq) ¹³¹I-labeled F6 F(ab')₂.

RIT Follow-Up

Tumor size and mouse body weight were measured initially twice a week and, after day 50, once a week. Three orthogonal diameters of the tumor were measured with a caliper, and tumor volume (V) was calculated by the formula:

$$V = (d_1 \times d_2 \times d_3)/2.$$

The mean time at which the tumors reached 6 times their initial volume was determined for the control groups. The growth delay (GD) was defined as the additional time a treated tumor needed to reach this volume. For hematologic toxicity assessment, peripheral white blood cells (WBCs) and platelets were counted on a MAXM counter (Coulter, Hialeah, FL) at 2, 4, 6, and 7 wk after therapy.

Whole-Body Cumulated Activity

For the AES 20/3.4, AES 48/3.7, hapten alone, and F(ab')₂ groups, whole-body counts for each mouse were measured on a Gammatome γ camera (Sopha Medical Vision, Buc, France) at 7 time points (1–26 d) using a pinhole collimator. Counts were corrected for background, isotope decay, and acquisition time. Whole-body count data for each group were fitted by least square regression to a sum of 3 exponentials (2 exponentials for the hapten alone and F(ab')₂ groups) and the area under the time–activity curve (MBq \times number of days) extrapolated to infinite time was calculated by integration of the fitted exponentials.

Immunohistochemistry

At the end of the 8-mo observation period, the animals were killed and dissected. The tumor nodule (if any), the major organs (liver, spleen, and lungs), and any macroscopically suspect organ were sampled for anatomopathologic examination. These specimens were fixed in 10% formalin, routinely processed, and embedded in paraffin. Sections (5 μ m) were obtained from the paraffin blocks and were immunostained for CEA and Ki-67 antigens, using the streptavidin-biotin-peroxidase complex and the diaminobenzidine chromogen (Immunotech). The sections were then counterstained with hematoxylin.

Statistical Analysis

Statistical analyses were performed on hematologic and clinical chemistry data and measurements of tumor GD. Global comparisons were made using the ANOVA procedure. Because of the limited number of animals, the nonparametric Mann-Whitney *U* test was used for pairwise comparisons.

RESULTS

Quality of Reagents

The F6–734 BsF(ab')₂ was 97% pure as assessed by gel-filtration chromatography. Its immunoreactivity was 90% on

an anti-F6-idiotype solid phase and 70% on a DTPA-In solid phase.

The labeling of the bivalent hapten with ¹³¹I was developed so that 2 iodine atoms could be substituted on the tyrosine residue of the peptide to achieve high specific activities (79 ± 12 MBq/mol). Although cysteamine was added to reduce radiolysis, immunoreactivity decreased from 96% to 87% during methanol removal (measured on an anti-DTPA-In solid phase after injections of mice were completed).

F6 F(ab')₂ was 90% pure as assessed by gel-filtration chromatography. ¹³¹I labeling of the F(ab')₂ yielded an average specific activity of 54 MBq/nmol, corresponding to 1.8–2.3 iodine atoms per molecule. The immunoreactivity measured on the anti-F6-idiotype solid phase after injections of mice were completed was 91%.

Whole-Body Cumulated Activity

Whole-body measurements showed that increasing the pretargeting time from 20 to 48 h was very effective at reducing the cumulated activity in the whole body (178 ± 16 and 71 ± 18 MBq × days, respectively). The cumulated activity for the directly labeled F(ab')₂ was found to be in the same range (105 ± 7 MBq × days). When the labeled bivalent hapten was injected alone, its rapid renal clearance accounted for a much smaller cumulated activity (8.8 ± 0.6 MBq × days).

RIT Side Effects

Mice Treated with the AES. For mice treated with an average activity of 3.8 MBq/g, treatment-related lethality depended on the pretargeting time (Table 1). In the 15/3.8 group, 50% of the animals died of hematologic toxicity between days 12 and 17 after treatment. Increasing the pretargeting time significantly reduced lethality; no death was recorded in the 48/3.7 group. All surviving animals in the 15/3.8 group presented with petechiae at 2 wk and thus were not assessed for hematology. In all other groups, the WBCs and platelets nadir was observed at 1 or 2 wk after treatment. WBC and platelet counts at the nadir were significantly lower (*P* < 0.01) in the 20/3.8 group compared with the 48/3.7 group. When comparing mice treated after 30- and 48-h pretargeting time, only platelet counts at the nadir were significantly different (*P* < 0.01, Table 1). For the 20-h time, the maximum tolerated dose (MTD), defined as the highest possible dose resulting in no treatment-related animal deaths, was 3.4 MBq/g or 96 MBq (Table 1). WBCs and platelets at the nadir did not significantly differ for the various activities administered (20/2.9, 20/3.4, and 20/3.8 groups). Interestingly, the treatment with 2.9 MBq/g at 20 h was significantly more myelosuppressive than was 3.7 MBq/g at 48 h (*P* < 0.01 for WBC and platelet counts at the nadir).

Body weight loss was not significantly different among all AES-treated groups. However, mice recovered their initial weight significantly more rapidly if they were treated with a low activity or if the pretargeting time was extended (20/2.9

TABLE 1
Toxicity of RIT

Parameter	AES 15/3.8	AES 30/3.9	AES 48/3.7	AES 20/2.9	AES 20/3.4	AES 20/3.8	F(ab') ₂	AES control	Hapten alone
No. of mice	10	12	12	12	12	12	10	9	8
Treatment-related deaths	5	2	0	0	0	1	2	0	0
Other	0	2	0	2	1	2	1	0	0
WBCs at nadir*†	NA	1.7 ± 0.7 (2.0)	2.1 ± 1.0 (2.0)	0.8 ± 0.6 (0.6)	0.9 ± 0.4 (1.0)	1.2 ± 0.5 (1.0)	1.4 ± 0.3 (1.4)	1.9 ± 1.2 (1.8)	6.3 ± 2.2 (5.7)
Platelets at nadir*‡	NA	0.5 ± 0.2 (0.5)	0.7 ± 0.2 (0.8)	0.5 ± 0.3 (0.5)	0.4 ± 0.2 (0.3)	0.3 ± 0.2 (0.3)	0.6 ± 0.2 (0.7)	0.3 ± 0.2 (0.3)	1.2 ± 0.1 (1.1)
% BW loss at nadir†	27 ± 8 (25)	25 ± 7 (25)	25 ± 9 (21)	23 ± 3 (22)	25 ± 9 (23)	26 ± 5 (25)	11 ± 8 (13)	13 ± 6 (14)	7 ± 3 (6)
BW recovery in d§	54 ± 26 (53)	108 ± 76 (73)	87 ± 43 (76)	35 ± 13 (26)	85 ± 54 (55)	124 ± 46 (143)	22 ± 15 (18)	26 ± 10 (25)	7 ± 6 (9)

*WBCs at nadir (10⁹/mm³); WBCs normal value, 6.87 ± 3.42 (10⁹/mm³); median value, 6.2 (10⁹/mm³).

†Mean ± SD; median value in parentheses.

‡Platelets at nadir (10⁹/mm³); platelets normal value, 1.33 ± 0.37 (10⁹/mm³); median value, 1.33 (10⁹/mm³).

§Time to initial BW recovery.

BW = body weight; NA = not assessable.

versus 20/3.8, $P < 0.01$; 20/3.8 versus 48/3.7, $P < 0.05$; Table 1).

The effect of AES nonspecific irradiation was tentatively assessed by injecting the same number of anti-CEA and anti-DTPA-In binding sites but carried by 2 distinct BsF(ab')₂, followed 15 h later by 3.6 MBq/g bivalent hapten (AES control). Lethality and toxicity in this group were lower compared with mice injected with the F6-734 BsF(ab')₂ under similar conditions (Table 1, 15/3.8 group). This is a consequence of the more rapid clearance of the G7A5-734 BsF(ab')₂ compared with the F6-734 BsF(ab')₂ (data not shown). For mice injected only with the labeled bivalent hapten (3.5 MBq/g), WBC and platelet counts remained normal and body weight loss did not differ from that of untreated mice (Table 1).

Mice Treated with ¹³¹I-Labeled F(ab')₂. Treatment with 2.7 MBq/g F6 F(ab')₂ fragment was above the MTD; 2 mice died of hematologic toxicity between days 7 and 13 after treatment (Table 1). It is noteworthy that mice treated with the F(ab')₂ (but not with the AES reagents) needed to have their thyroid blocked; otherwise dramatic lethality was observed. The hematologic toxicity induced by the F(ab')₂, as measured on surviving mice, was equivalent to most AES treatments, with the exception of the 20/3.4 and 20/3.8 groups ($P < 0.05$ for platelets, Table 1). Mice treated with the F(ab')₂ lost significantly less weight compared with any AES-treated mice ($P < 0.01$).

Tumor Growth Control

Mice Treated with the AES. Treatment with any of the AES protocols resulted in substantial control of the tumor growth. Nonspecific irradiation (AES control) induced a GD of 16 d (Table 2). For mice treated with the specific reagents, the level of tumor growth control depended on the pretargeting time and the injected activity (Table 2). No tumor relapse was observed with the 15-h pretargeting time (Fig. 1A, Table 2). In the 30/3.9 group, 1 tumor was probably progressing when the mouse died of infection (Fig. 1B). As the pretargeting time was lengthened to 48 h, all tumors except 2 relapsed (GD, 82 ± 26 d; Table 2, Fig. 1C). For the 20-h

pretargeting time, 2 tumors relapsed at the lowest activity dose (2.9 MBq/g, GD of 161 and 197 d), 1 relapsed at the highest activity (3.9 MBq/g, GD 164 d), and none relapsed at the intermediate activity (Figs. 2A-C, Table 2). When compared with untreated tumors, the doubling time of relapsing tumors was significantly longer (7.6 ± 3.0 d versus 3.6 ± 1.0 d, $P < 0.01$).

Mice Treated with ¹³¹I-Labeled F(ab')₂. All tumors of mice treated with F6 F(ab')₂ relapsed, with a mean GD significantly shorter ($P < 0.01$) than that of the AES 48/3.7 group (Table 2, Fig. 3A).

Health Status of Surviving Treated Animals

Surviving mice (i.e., AES-treated mice) were killed 8 mo after treatment. At that time, all animals had gained in body weight (mean body weight, 31.5 ± 3.4 g). Renal and liver functions were assessed by clinical chemistry analysis. Serum samples were analyzed for urea, creatinine, glutamic oxaloacetic transaminase (GOT), glutamic pyruvic transaminase (GPT), alkaline phosphatase, and bilirubin. Mice from the AES 48/3.7 group had elevated GOT but did not have elevated GPT, suggesting muscular stress at the time of killing rather than altered liver functions. In the AES 30/3.9 group, both urea and creatinine values were elevated with respect to normal values (urea, 0.73 ± 0.15 g/L versus 0.55 ± 0.1 g/L, $P = 0.02$; creatinine, 5.1 ± 1.6 mg/L versus 3.7 ± 0.5 mg/L, $P = 0.07$). This possible alteration of the glomerular filtration, although moderate, was not observed in the AES 20/3.8 group treated with the same level of activity. Mice from the other groups had chemistry values within the normal range.

Anatomopathologic Examination

Neither micrometastasis nor radioinduced lesions were detected in any of the organs sampled. However, microabscesses were found in some liver sections; hyperplasia was found in some spleen, kidney, and colon samples; and some lung samples were inflammatory. These observations may be related to a lack of a sepsis during the 8-mo survey of the immunodeficient mice. On microscopic examination, regrow-

TABLE 2
Efficiency of RIT

Parameter	AES 15/3.8 (%)	AES 30/3.9 (%)	AES 48/3.7 (%)	AES 20/2.9 (%)	AES 20/3.4 (%)	AES 20/3.8 (%)	F(ab') ₂	AES control
Assessable animals (n)	5	8	12	12	11	10	7	9
Tumor disappearance (n)	1	3	1	7	1	2	0	0
Tumor regression* (n)	4	3	0	3	7	5	0	0
Tumor stabilization† (n)	0	2	1	0	3	2	0	0
Tumor progression (n)	0	0	10	2	0	1	7	9
GD (d)	—	—	50-137	197 and 161	—	164	48 ± 13‡	16 ± 7‡
Cured animals (n)	2/5 (40)	4/8 (50)	1/12 (8)	7/12 (58)	1/11 (9)	4/10 (40)	None	None

*Shrinkage to <50% of initial volume.

†Stabilization between half and twice initial volume.

‡Mean ± SD.

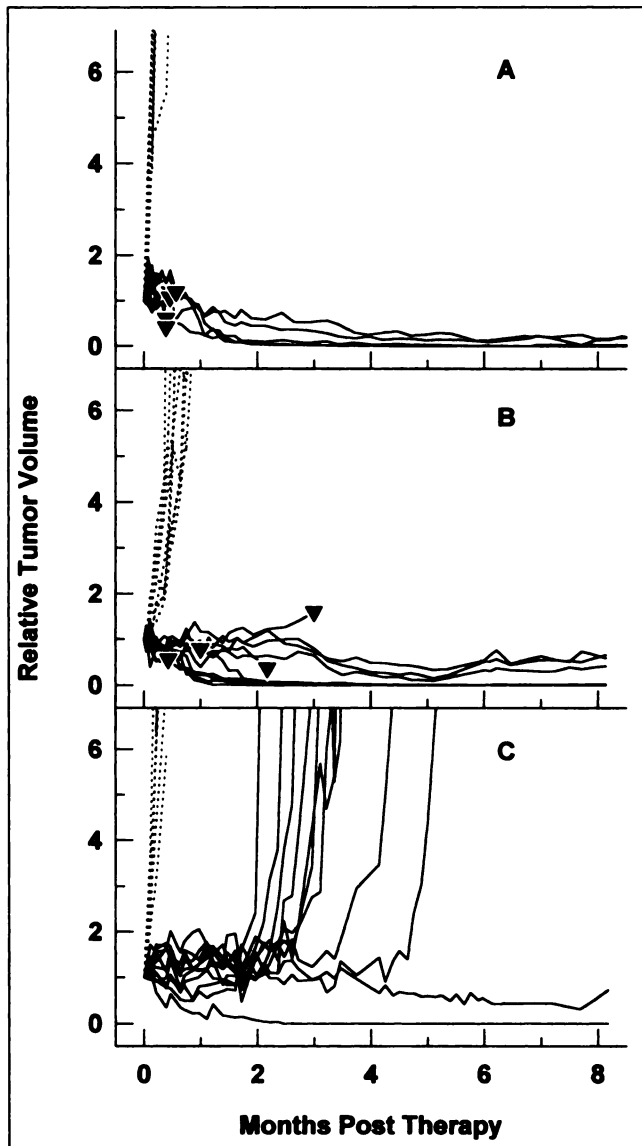


FIGURE 1. Comparison of AES RIT for various pretargeting delays. Ratio of current tumor volume to tumor volume at time of treatment for individual mice is shown. Mice were injected with almost constant activity of ^{131}I -labeled bivalent hapten at selected time intervals after administration of $\text{BsF}(\text{ab}')_2$ by various pretargeting delays. (A) 15 h, AES 15/3.8 group. (B) 30 h, AES 30/3.9 group. (C) 48 h, AES 48/3.7 group. Treated mice = —; untreated mice = - - -; death of mouse (\blacktriangledown).

ing tumors (e.g., from the AES 48/3.7 group) were found similar to untreated tumors. Neoplastic cells were small and very undifferentiated with numerous mitotic figures (Figs. 4A and B). By contrast, the morphology of neoplastic cells from residual nodules in mice with stabilized tumors was different (Figs. 4C and D). Cells had multilobular nuclei, numerous mucous vacuoles in the cytoplasm, and a low nucleus-to-cytoplasm ratio. No mitoses were seen. Moreover, some clusters presented with glandular lumen, suggesting a more differentiated status. CEA was mainly expressed at the cell membrane in regrowing and untreated tumors, as well as in 42% of the residual nodules. In the other 58%,

CEA labeling was exclusively cytoplasmic. In regrowing tumors, Ki-67 antigen immunostaining was intense, showing actively cycling cells, whereas the staining was negative in all but 1 of the stabilized nodules.

Cure Rates

Mice were considered cured if the tumor had completely disappeared or if the residual nodule was found tumor free by histologic examination and no metastatic site was found macroscopically at dissection or by histologic examination of liver, spleen, and lungs. Under those criteria, the overall cure rate of AES RIT was 33%, and cure rates for individual groups ranged from 8% to 58% (Table 2).

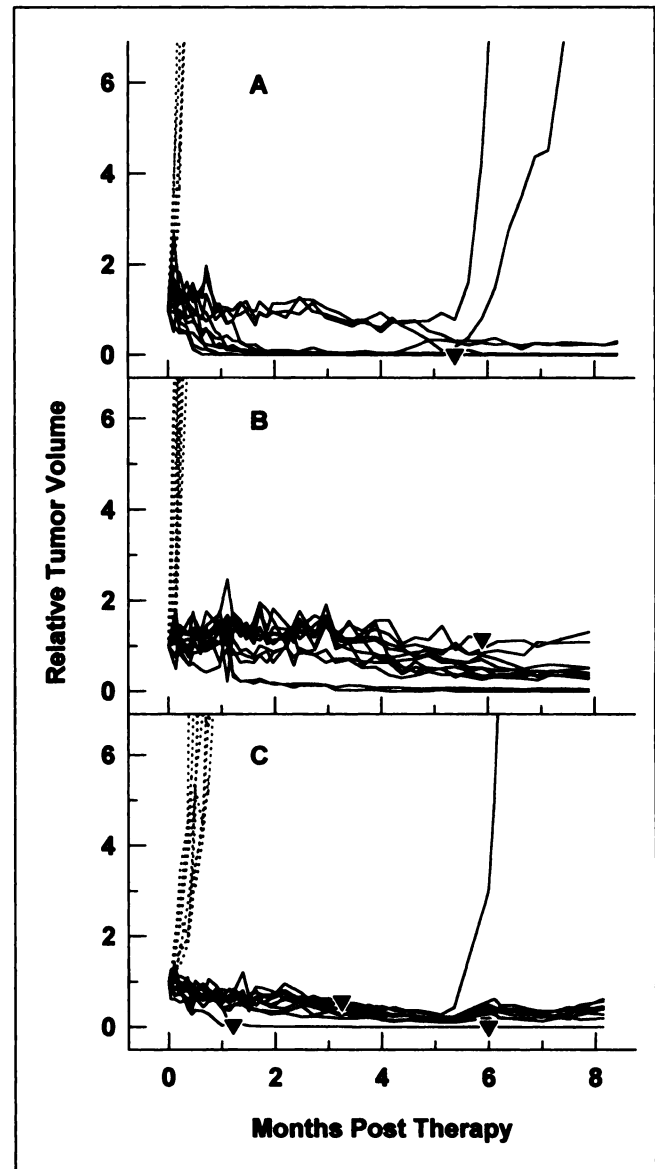


FIGURE 2. AES RIT with various activities of ^{131}I -labeled bivalent hapten. Mice were injected with $\text{BsF}(\text{ab}')_2$ and 20 h later with mean activities of 2.9, 3.4, and 3.8 MBq/g. (A) AES 20/2.9 group. (B) AES 20/3.4 group. (C) AES 20/3.8 group. Treated mice = —; untreated mice = - - -; death of mouse (\blacktriangledown).

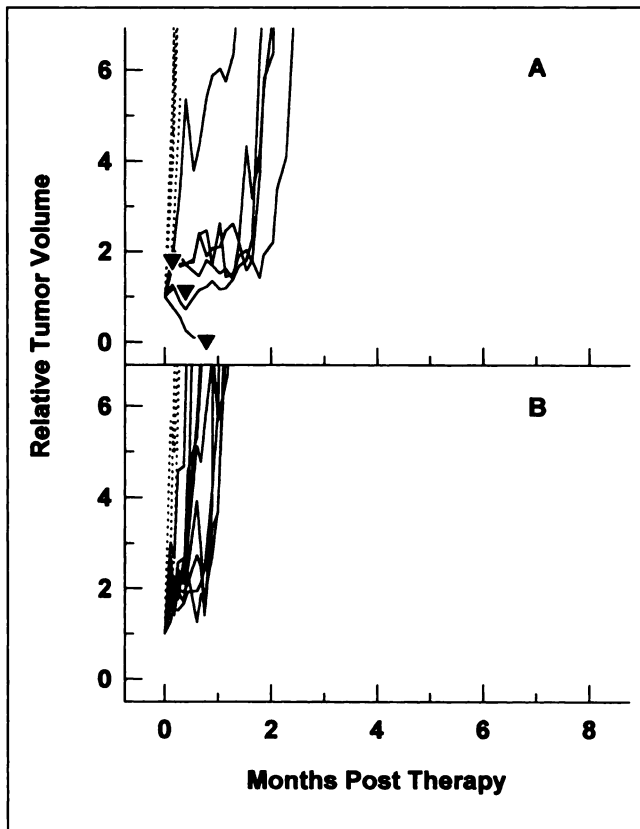


FIGURE 3. RIT with ¹³¹I-labeled anti-CEA F(ab')₂ and nonspecific AES RIT. (A) Treatment with 3.8 MBq/g ¹³¹I-labeled F(ab')₂. (B) AES control group. Mice were injected with molar mixture of anti-CEA and anti-DTPA-In BsF(ab')₂ and 15 h later with mean activity of 3.6 MBq/g ¹³¹I-labeled bivalent hapten. Treated mice = —; untreated mice = - - -; death of mouse (▼).

DISCUSSION

Previous biodistribution studies (12) in the LS174T tumor model have shown that the saturation of the tumor was obtained by injecting 5 nmol (500 µg) BsF(ab')₂ and that the pretargeted BsF(ab')₂ was saturated by the injection of 0.5 mol bivalent hapten per mol antibody. ¹³¹I dosimetry calculation based on biodistribution data obtained for 1 nmol BsF(ab')₂, 20-h pretargeting time, and 0.5 nmol ¹²⁵I-labeled bivalent hapten predicted the delivery of 32 ± 16 Gy to the tumor. However, it is commonly accepted that doses in the 60- to 90-Gy range should be delivered to solid tumors to achieve antitumor activity (19). Thus, to deliver sufficient radiation doses with the AES reagents to the tumor, BsF(ab')₂ and bivalent hapten administered amounts were increased 3-fold (3 and 1.5 nmol, respectively) in these RIT experiments.

The results reported here clearly show substantial tumor growth control over a period of 8 mo and a 33% cure rate after a single injection of ¹³¹I-labeled bivalent hapten administered 20 h after anti-CEA × anti-hapten BsF(ab')₂. Interestingly, after irradiation, tumor cells found in stabilized nodules had moved from an undifferentiated and highly proliferative status to a more differentiated and low

proliferation state. These histopathologic changes are consistent with previously described changes in tissues exposed to high-dose radiation (20). The treatment efficiency and related toxicity of AES RIT were modulated by the pretargeting time. The labeled bivalent hapten was highly myelosuppressive when injected 15 h after BsF(ab')₂ but was well tolerated when injected at 20 h. Increasing the pretargeting time to 48 h and keeping the treatment activity constant resulted in a lower tumor growth control, although still more potent than the treatment with ¹³¹I-labeled IgG (21) and F(ab')₂.

In the LS174T model, tumor relapse has been reported 50–60 d after treatment with ¹³¹I-labeled IgG (22–24), and treatment with 2 injections of 55.5 MBq ¹³¹I-labeled F(ab')₂ has been reported to induce a GD of 40 d (24). Our data relative to the efficiency and toxicity of ¹³¹I-labeled IgG (21) and F(ab')₂ are in good agreement with these results. Attempts to improve the therapeutic outcome have been made by experimentally combining RIT with radiotherapy (24), chemotherapy (25), or other modalities such as tumor blood flow-modifying agents (23). RIT with second-generation high-affinity labeled antibodies (26) (K_d lower than 0.1 nmol/L) targeting the more highly expressed antigen TAG-72 (27) has also been considered. When compared with all of these strategies, AES RIT achieved higher cure rates.

With the AES, increasing the pretargeting time significantly reduced the cumulated activity in the whole body. These results confirmed our original biodistribution studies with 48-h pretargeting time showing a better selectivity as a consequence of the reduced amount of circulating bivalent hapten associated with BsF(ab')₂ (12). Thus, increasing the pretargeting time significantly reduced myelotoxicity, which depends on the level of circulating activity. However, the body weight loss was more pronounced and extended after AES treatment (even for the 48-h pretargeting time in the 48/3.7 group) compared with F(ab')₂ despite the fact that cumulated activity was slightly lower. We suggest that the stability of the labeling of the bivalent hapten, an advantage with respect to tumor irradiation, may account for low but long-lasting normal tissue irradiation. On the other hand, the labeled F(ab')₂ was more rapidly dehalogenated as assessed by the faster whole-body activity clearance and the requirement for thyroid saturation before treatment.

Biodistributions with the AES reagents have shown a rapid renal excretion of the excess of bivalent hapten and a significant uptake in the kidneys at late time points when compared with F(ab')₂ (0.31 ± 0.09 versus 0.06 ± 0.02 percentage injected dose/g at 4 d) (12). No radioinduced lesions were identified by anatomopathologic examination of the kidneys at the end of the 8-mo follow-up period. Signs of a possible mild renal toxicity were observed only for mice from the AES 30/3.9 group. This was not observed in the AES 20/3.8 group treated with the same level of activity. Several experimental studies have shown that the administration of positively charged amino acids (e.g., lysine) could

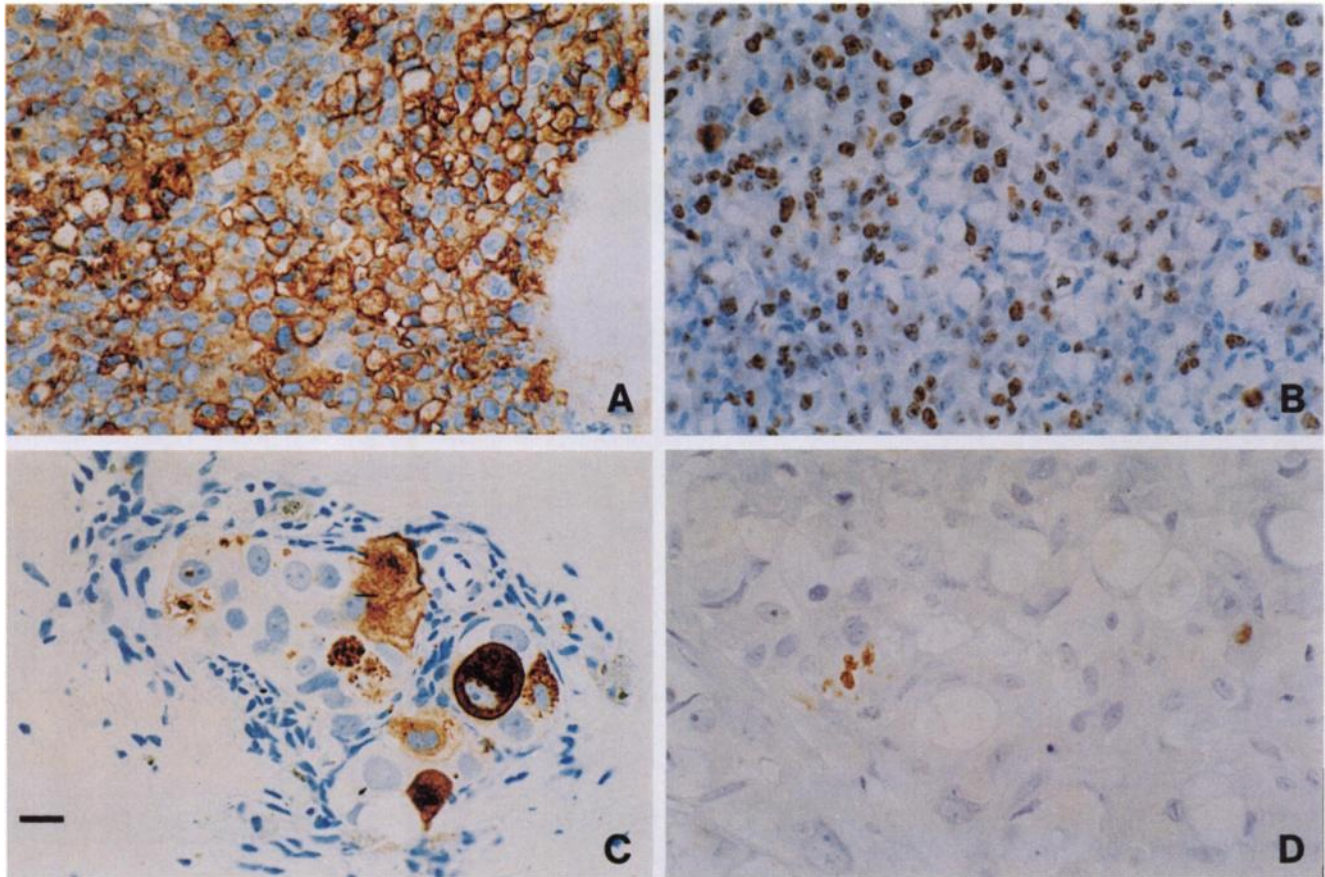


FIGURE 4. Immunohistochemistry of LS174T xenografts after AES RIT. Tumor sections were immunostained with anti-CEA (A and C) and anti-Ki-67 antibodies (B and D). (A and B) Regrowing tumor from AES 48/3.7 group. (C and D) Residual nodule from mouse with stabilized tumor from AES 15/3.8 group. Bar = 25 μ m.

block renal tubular uptake of antibody fragments labeled with various isotopes, including ^{131}I (28,29). A similar approach may be used with AES to prevent kidney toxicity.

It is likely that repeating treatment after recovery from myelosuppression will be necessary to achieve high therapeutic efficiency. This requires continuous expression of the target antigen by the neoplastic cell. Unlike previously reported results on LS174T (30), immunohistochemistry analysis showed that AES RIT did not select an antigen-negative cell population either in relapsing tumors or in remaining nodules. However, the susceptibility to CEA-targeted RIT of cells such as those found in the remaining nodules is more speculative, because CEA seemed to be expressed mostly in the cytoplasm of some of these cells.

In the clinic, a dosimetry study in patients with medullary thyroid cancer (MTC) and small cell lung cancer (16) has shown that AES pretargeting could achieve high absorbed doses (0.5–47 Gy/GBq), especially for small MTC recurrences. With the help of bone marrow support, doses of ^{131}I -labeled immunoglobulin G up to 26 GBq have been administered. AES should be able to deliver therapeutically useful radiation to tumor cells in the clinic. Preliminary clinical trials show that objective responses are obtained in the 3- to 8-GBq dose range without unmanageable toxicity.

CONCLUSION

These clinical results suggest, in addition to the therapeutic efficiency of AES RIT in this experimental model, that treatments with activities in the range of those already used with conventional RIT in solid tumors (4,6,31,32) should achieve significant antitumor effects in patients.

ACKNOWLEDGMENTS

This work was supported in part by “Saut Technologique” grant 92C 0429 from the French Ministry of Research and Technology. The authors thank Dr. Françoise Bertault-Peres for careful management of the hematologic and clinical chemistry analysis.

REFERENCES

1. Press OW, Eary JF, Appelbaum FR, et al. Phase II trial of I-131-B1 (anti-CD20) antibody therapy with autologous stem cell transplantation for relapsed B cell lymphomas. *Lancet*. 1995;346:336–340.
2. Wahl RL, Zasadny KR, MacFarlane D, et al. Iodine-131 anti-B1 antibody for B-cell lymphoma: an update on the Michigan Phase I experience. *J Nucl Med*. 1998;39(suppl):21S–27S.
3. Lane DM, Eagle KF, Begent RHJ, et al. Radioimmunotherapy of metastatic colorectal tumours with iodine-131-labelled antibody to carcinoembryonic antigen: phase I/II study with comparative biodistribution of intact and F(ab')₂ antibodies. *Br J Cancer*. 1994;70:521–525.

4. Crippa F, Bolis G, Seregini E, et al. Single-dose intraperitoneal radioimmunotherapy with the murine monoclonal antibody I-131 MOv18: clinical results in patients with minimal residual disease of ovarian cancer. *Eur J Cancer*. 1995;31A:686-690.
5. Juweid M, Sharkey RM, Behr TM, et al. Clinical evaluation of tumor targeting with the anticarcinoembryonic antigen murine monoclonal antibody fragment, MN-14 F(ab)₂. *Cancer*. 1996;78:157-168.
6. Behr TM, Sharkey RM, Juweid ME, et al. Phase I/II clinical radioimmunotherapy with an iodine-131-labeled anti-carcinoembryonic antigen murine monoclonal antibody IgG. *J Nucl Med*. 1997;38:858-870.
7. Ratliff B, Reno J, Axworthy D, et al. Performance of antibody streptavidin pretargeting in patients: initial results [abstract]. *J Nucl Med*. 1995;36:225P.
8. Paganelli G, Orecchia R, Jereczek-Fossa B, et al. Combined treatment of advanced oropharyngeal cancer with external radiotherapy and three-step radioimmunotherapy. *Eur J Nucl Med*. 1998;25:1336-1339.
9. Le Doussal JM, Gruaz-Guyon A, Martin M, Gautherot E, Delaage M, Barbet J. Targeting of indium-111-labeled bivalent hapten to human melanoma mediated by bispecific monoclonal antibody conjugates: imaging of tumors hosted in nude mice. *Cancer Res*. 1990;50:3445-3452.
10. Manetti C, Rouvier E, Gautherot E, Loucif E, Barbet J, Le Doussal JM. Targeting BCL₂ lymphoma with anti-idiotypic antibodies: biodistribution kinetics of directly labeled antibodies and bispecific antibodytargeted bivalent haptens. *Int J Cancer*. 1997;71:1000-1009.
11. Janevik-Ivanovska E, Gautherot E, Hilaiet de Boisferon M, et al. Bivalent hapten peptides designed for iodine-131 pretargeted radioimmunotherapy. *Bioconj Chem*. 1997;8:526-533.
12. Gautherot E, Le Doussal JM, Bouhou J, et al. Delivery of therapeutic doses of radioiodine using bispecific antibody-targeted bivalent haptens. *J Nucl Med*. 1998;39:1937-1943.
13. Le Doussal JM, Chetanneau A, Guyon-Gruaz A, et al. Bispecific monoclonal antibody-mediated targeting of an indium-111-labeled DTPA dimer to primary colorectal tumors: pharmacokinetics, biodistribution, scintigraphy and immune response. *J Nucl Med*. 1993;34:1662-1671.
14. Vuillez JP, Moro D, Bricchon PY, et al. Two-step immunoscintigraphy for non-small-cell lung cancer staging using a bispecific anti-CEA/anti-indium-DTPA antibody and an indium-111-labeled DTPA dimer. *J Nucl Med*. 1997;38:507-511.
15. Barbet J, Peltier P, Bardet S, et al. Radioimmunodetection of medullary thyroid carcinoma using indium-111 bivalent hapten and anti-CEA × anti-DTPA-indium bispecific antibody. *J Nucl Med*. 1998;39:1172-1178.
16. Bardies M, Bardet S, Faivre-Chauvet A, et al. Bispecific antibody and iodine-131-labeled bivalent hapten dosimetry in patients with medullary thyroid or small-cell lung cancer. *J Nucl Med*. 1996;37:1853-1859.
17. Morel A, Darmon M, Delaage M. Recognition of imidazole and histamine derivatives by monoclonal antibodies. *Mol Immunol*. 1990;27:995-1000.
18. Glennie MJ, McBride HM, Worth AT, Stevenson GT. Preparation and performance of bispecific F(ab'γ)₂ antibody containing thioether-linked Fab' γ fragments. *J Immunol*. 1987;139:2367-2375.
19. Buchsbaum DJ, Langmuir VK, Wessels BW. Experimental radioimmunotherapy. *Med Phys*. 1993;20:551-567.
20. Robbins SL, Cotran RS, Kumar V. *Pathologic Basic of Disease*. 3rd ed. Philadelphia, PA: WB Saunders; 1984:466-467.
21. Gautherot E, Bouhou J, Le Doussal JM, et al. Therapy for colon carcinoma xenografts with bispecific antibody-targeted iodine-131-labeled bivalent hapten. *Cancer*. 1997;80(suppl):2618-2623.
22. Blumenthal RD, Sharkey RM, Natale AM, Kashi R, Wong G, Goldenberg DM. Comparison of equitoxic radioimmunotherapy and chemotherapy in the treatment of human colonic cancer xenografts. *Cancer Res*. 1994;54:142-151.
23. Pedley RB, Boden JA, Boden R, et al. Ablation of colorectal xenografts with combined radioimmunotherapy and tumor blood flow-modifying agents. *Cancer Res*. 1996;56:3293-3300.
24. Buchegger F, Rojas A, Bischof-Delaloye A, et al. Combined radioimmunotherapy and radiotherapy of human colon carcinoma grafted in nude mice. *Cancer Res*. 1995;55:83-89.
25. Tschmelitsch J, Barendsward E, Williams C Jr, et al. Enhanced antitumor activity of combination radioimmunotherapy (¹³¹I-labeled monoclonal antibody A33) with chemotherapy (fluorouracil). *Cancer Res*. 1997;57:2181-2186.
26. Schlom J, Eggensperger D, Colcher D, et al. Therapeutic advantage of high-affinity anticarcinoma radioimmunoconjugates. *Cancer Res*. 1992;52:1067-1072.
27. Greiner JW, Ullmann CD, Nieroda C, et al. Improved radioimmunotherapeutic efficacy of an anticarcinoma monoclonal antibody (¹³¹I-CC49) when given in combination with gamma-interferon. *Cancer Res*. 1993;53:600-608.
28. Behr TM, Sharkey RM, Juweid ME, et al. Reduction of the renal uptake of radiolabeled monoclonal antibody fragments by cationic amino acids and their derivatives. *Cancer Res*. 1995;55:3825-3834.
29. Behr TM, Goldenberg DM, Becker W. Reducing the renal uptake of radiolabeled antibody fragments and peptides for diagnosis and therapy: present status, future prospects and limitations. *Eur J Nucl Med*. 1998;25:201-212.
30. Esteban JM, Hyams DM, Beatty BG, Merchant B, Beatty D. Radioimmunotherapy of human colon carcinomatosis xenograft with ⁹⁰Y-ZCE025 monoclonal antibody: toxicity and tumor phenotype studies. *Cancer Res*. 1990;50(suppl):989s-992s.
31. Meredith RF, Bueschen AJ, Khazaeli MB, et al. Treatment of metastatic prostate carcinoma with radiolabeled antibody CC49. *J Nucl Med*. 1994;35:1017-1022.
32. Juweid M, Sharkey RM, Behr T, et al. Radioimmunotherapy of medullary thyroid cancer with iodine-131-labeled anti-CEA antibodies. *J Nucl Med*. 1996;37:905-911.